# THE TREATMENT OF THE THROTTLING EFFECT IN INCOMPRESSIBLE 1D FLOW SOLVERS

C. Fleming, G. Clark, K. Meeks; Atkins Ltd, UK
T. Wicht; HBI Haerter, Switzerland

## ABSTRACT

This paper is concerned with the throttling effect of a tunnel fire and how it is treated in one-dimensional flow solvers. We explain the primary mechanisms by which airflow is resisted by a tunnel fire. While compressible flow solvers inherently capture these mechanisms, corrections are required for incompressible solvers. In one approach, where a user-controlled parameter is required, we suggest a method for its reliable calculation.

*Keywords: fire throttling effect, tunnel fire, incompressible flow solver, longitudinal ventilation system*

## 1.    INTRODUCTION

When a fire occurs in a uni-directional tunnel with a longitudinal ventilation system, the ventilation system is typically used to direct combustion products towards the exit portal, away from trapped vehicles. This aids self-rescue of tunnel users and enables fire fighters to tackle the fire from the upstream side.

A longitudinal ventilation system is typically designed to induce an airflow at such a rate as to prevent reverse stratification, or backlayering, of smoke upstream of the fire site. There are several established models for predicting the 'critical velocity', the velocity threshold above which backlayering does not occur (e.g. Oka and Atkinson, 1995; Kennedy et al, 1996). The ventilation system must introduce sufficient momentum to achieve the critical velocity while overcoming several sources of aerodynamic resistance, for example due to vehicle drag, wall friction, local losses, buoyancy, portal pressure differences and the momentum change across the fire. While the critical velocity reaches a plateau for heat release rates above a certain threshold (Hwang and Edwards, 2005), the aerodynamic resistance continues to increase (Vaitkevicius et al, 2015).

In this paper we examine the primary mechanisms of fire throttling, and show how they are treated in incompressible one-dimensional flow solvers. We review two models of the momentum change across the fire, and propose a method for their implementation in a particular type of flow solver.

## 2.    ANALYSIS OF FIRE THROTTLING

### 2.1.    Primary mechanisms

Hwang and Chaiken (1978) identified the primary mechanisms of fire-related resistance in their investigation into the interaction of fires and ventilation flow rate in mine shafts. The flow is heated as it passes through the fire, resulting in a reduction in density and increase in velocity downstream. Wall friction and local losses increase downstream of the fire, as they are proportional to density and to the square of velocity, and the latter dominates. Additionally, the fluid momentum increases as it passes the fire, presenting a corresponding resistance to the upstream flow. Hwang and Chaiken also allow for mass injection due to combustion, which is not considered in this paper.

## 2.2. Fire throttling in incompressible flow solvers

One-dimensional incompressible flow solvers are based on the Bernoulli equation, with additional terms to account for energy sources and losses. The flow velocity is typically calculated by balancing the pressure changes due to fans, vehicles, wall friction, local losses, buoyancy, etc. (US Department of Transportation, 2001).

### 2.2.1. Wall friction and local losses

Wall friction and local losses are normally determined by applying a local loss factor (*K*-factor) to the local dynamic pressure,

$$\Delta p = K \frac{1}{2} \rho u^2 \tag{1}$$

where $\rho$ is density and $u$ is velocity. The loss factor corresponding to wall friction is calculated as $K_f = \lambda L/D$, where $\lambda$ is the Darcy friction factor and $L$ and $D$ are the length and hydraulic diameter of the tunnel. In regions of elevated temperature, for example downstream of a fire, the density and velocity of the heated air is calculated by applying the Ideal Gas Law,

$$\rho_h = \rho_c \frac{T_c}{T_h} \tag{2}$$

$$u_h = u_c \frac{T_h}{T_c} \tag{3}$$

where $T_c$ and $T_h$ are the absolute temperatures (in Kelvin) upstream ('cold') and downstream ('hot') respectively. Equations 1 – 3 are combined to yield the corrected loss,

$$\Delta p = K \frac{1}{2} \rho u^2 \frac{T_h}{T_c} \tag{4}$$

Note that wall friction and local losses diminish with distance from the fire, as the downstream air loses heat to the tunnel walls.

### 2.2.2. Momentum change across the fire

As the flow passes the fire it is heated and undergoes rapid expansion. This change of velocity and density constitutes an increase in momentum, which resists the upstream flow. This mechanism is not captured in the Bernoulli equation or the usual local losses, and hence must be represented with a further loss term.
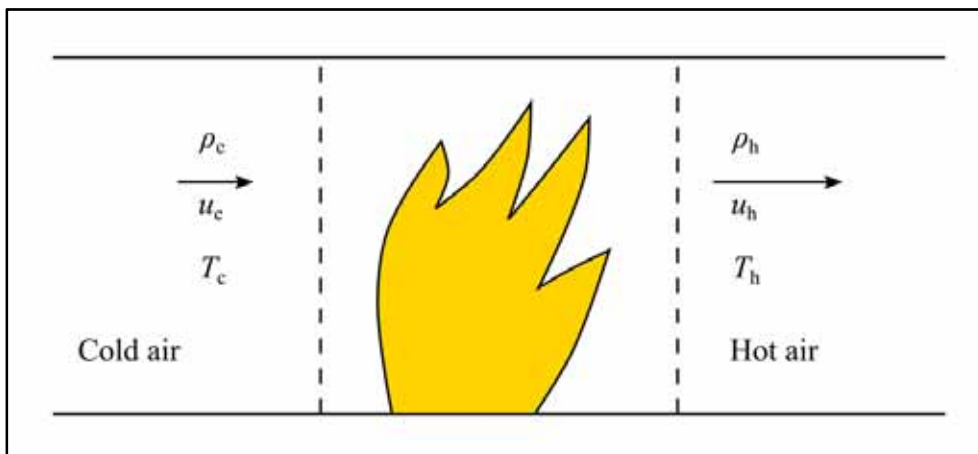


**Figure 1:** Diagram of the control volume around the fire, with flow from left to right

This term can be calculated following Hwang and Chaiken (1978), who consider a one-dimensional control volume containing a fire in a tunnel, with the ventilation system driving an airflow in one direction. The scenario is illustrated in figure 1, where heat is added to the flow as it passes the fire, reducing the density and increasing the velocity downstream. The resistance to the upstream flow is equivalent to the change of momentum,

$$\begin{aligned} F &= \dot{m}(u_c - u_h) \\ &= \rho_c u_c A (u_c - u_h) \end{aligned} \tag{5}$$

The downstream velocity is expressed in terms of the upstream velocity by applying a temperature correction based on the Ideal Gas Law (equation 3), yielding the pressure drop across the fire,

$$\Delta p_{\text{fire}} = \frac{F}{A} = \rho u_c^2 \left( \frac{T_h}{T_c} - 1 \right) \tag{6}$$

Another method of predicting this loss term is presented by Dutrieue and Jacques (2006), who derive an empirical relationship between the fire pressure drop, heat release rate, hydraulic diameter and upstream velocity, based on a parametric study using a three-dimensional flow solver,

$$\Delta p_{\text{fire}} = \frac{Q^{0.8} u^{1.5}}{D^{1.5}} C \tag{7}$$

where $C$ is an empirical constant with a value of $41.5 \times 10^{-6}$.

## 3. IMPLEMENTATION OF MOMENTUM CHANGE AT FIRE

Some incompressible flow solvers allow the user to specify the pressure change at the fire as an input value. This can be useful where additional effects, for example the deflection of the fire plume, are to be accounted for. We demonstrate how this feature can be used in one such solver, IDA Tunnel 1.1 (EQUA, 2014). We implement the Hwang and Chaiken model (equation 6) and the Dutrieue and Jacques model (equation 7), hereafter referred to as HC78 and DJ06 respectively. Predictions of flow velocity and static pressure are then compared with results from SES v4.1, which uses the HC78 model without user input.

### 3.1. Fire pressure change coefficient

In IDA Tunnel, the pressure change at the fire site is specified using a coefficient, $C_{\text{fire}}$, which acts as a constant of proportionality to the heat release rate. This coefficient can be determined by applying the HC78 or DJ06 models.

As both models require knowledge of the flow solution, they must be applied iteratively. An initial flow is simulated with $C_{\text{fire}} = 0$ Pa/MW. The value of $C_{\text{fire}}$ is then updated by calculating the fire pressure change (via the HC78 or DJ06 model) and dividing by the heat release rate,

$$C_{\text{fire}} = \frac{\Delta p_{\text{fire}}}{Q} \tag{8}$$

The simulation is then repeated with the updated value of $C_{\text{fire}}$, and the procedure is continued iteratively until the terms in the fire pressure change equation (e.g. equation 6 for HC78 or equation 7 for DJ06) converge.
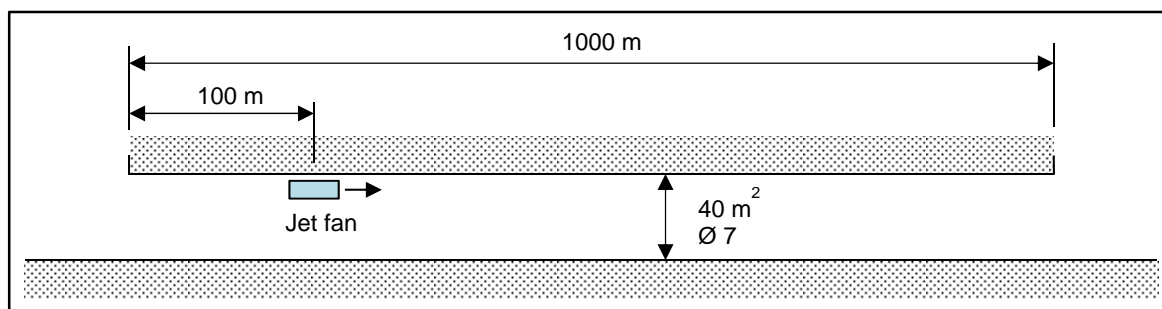
## 3.2. Solver verification



**Figure 2:** Diagram of the tunnel showing primary dimensions for verification simulations

Prior to evaluating the implementation of the HC78 and DJ06 models in IDA Tunnel 1.1 against SES 4.1, we consider a trivial scenario without a fire to verify agreement of the solvers. A single jet fan is simulated in an empty 1 km long tunnel, as described in figure 2 and table 1.

Adiabatic walls are specified[1] and local losses are neglected in order to isolate the pressure drop at the fire site in later simulations. The tunnel is discretised with a one-dimensional grid of 8 m long elements. In SES, two 'sections' are created: the first extending from the inlet to the 200 m point and containing the jet fan at 100 m, and the second section between the 200 m point and the exit portal.

**Table 1:** Model parameters for verification simulations

| | | |
|---|---|---|
| Ambient conditions | Temperature | 10°C |
| | Absolute atmospheric pressure | 101325 Pa |
| Tunnel | Length | 1000 m |
| | Cross-sectional area | 40 m$^2$ |
| | Hydraulic diameter | 7 m |
| | Gradient | 0% |
| | Darcy friction factor | 0.02 |
| Ventilation system | Number of jet fans | 1 |
| | Position | 100 m from entry portal |
| | Cross-sectional area | 1 m$^2$ |
| | Jet velocity | 30 m s$^{-1}$ |
| | Installation factor | 1.0 |

Predictions of the flow velocity and the total pressure change over the downstream section (between the 200 m point and the exit portal) by IDA Tunnel and SES agree well, as shown in table 2.

**Table 2:** Predictions of velocity and total pressure change in the absence of a fire

| Solver | Velocity [m s$^{-1}$] | Total pressure change (200 m $< x <$ 1000 m) [Pa] |
|---|---|---|
| SES | 3.702 | 19.704 |
| IDA | 3.701 | 19.670 |

---

[1]This required the wall heat transfer variable 'QWALSS' in the SES source code to be set to zero.

### 3.3. Predictions of the pressure change at the fire

A fire is now introduced in the region between 200 m and 208 m from the entry portal, so that it is downstream of the jet fan. The convective heat release rate is 20 MW, with no radiative portion and no mass generation. All other simulation conditions are consistent with the preceding verification case.

Note that the prescription of adiabatic walls is unphysical, leading to the over-prediction of wall friction and local losses (neglected here) downstream as the air is not allowed to lose heat. However, this measure eliminates differences due to the wall heat transfer models in IDA Tunnel and SES v4.1 and hence the predicted momentum change at the fire site can be compared directly.

Three cases are simulated using IDA Tunnel: firstly with the coefficient $C_{\text{fire}}$ set to zero, and two further cases where $C_{\text{fire}}$ is set according to the HC78 and DJ06 models as outlined in section 3.1. The method of implementation of these models in IDA is verified by comparison with an SES simulation, as this solver uses the HC78 model without user input.

Longitudinal profiles of static pressure, velocity and temperature are presented in figure 3. Note that this scenario is devised specifically for comparing predictions of the pressure drop at the fire site. The adiabatic condition at the walls and elimination of entry and exit losses mean that the numerical values reported cannot be applied to other tunnel fire cases.

No pressure drop occurs across the fire for the $C_{\text{fire}} = 0$ case. However, the increase in wall friction downstream of the fire is clearly indicated by the change in static pressure gradient at $x = 200$ m. As explained in section 2.2.1, this is because the greater downstream temperature corresponds to reduced density and increased velocity.

Predictions of static pressure, velocity and temperature by IDA Tunnel using the HC78 model agrees perfectly with SES, verifying the implementation method. Note that static pressure is only available at a single point in SES – the node at $x = 200$ m, between the upstream and downstream sections.

The DJ06 model over-predicts the pressure drop at the fire site relative to the HC78 model. The greater system resistance reduces the flow velocity, which in turn increases the heat transfer from the fire, leading to a higher downstream temperature.
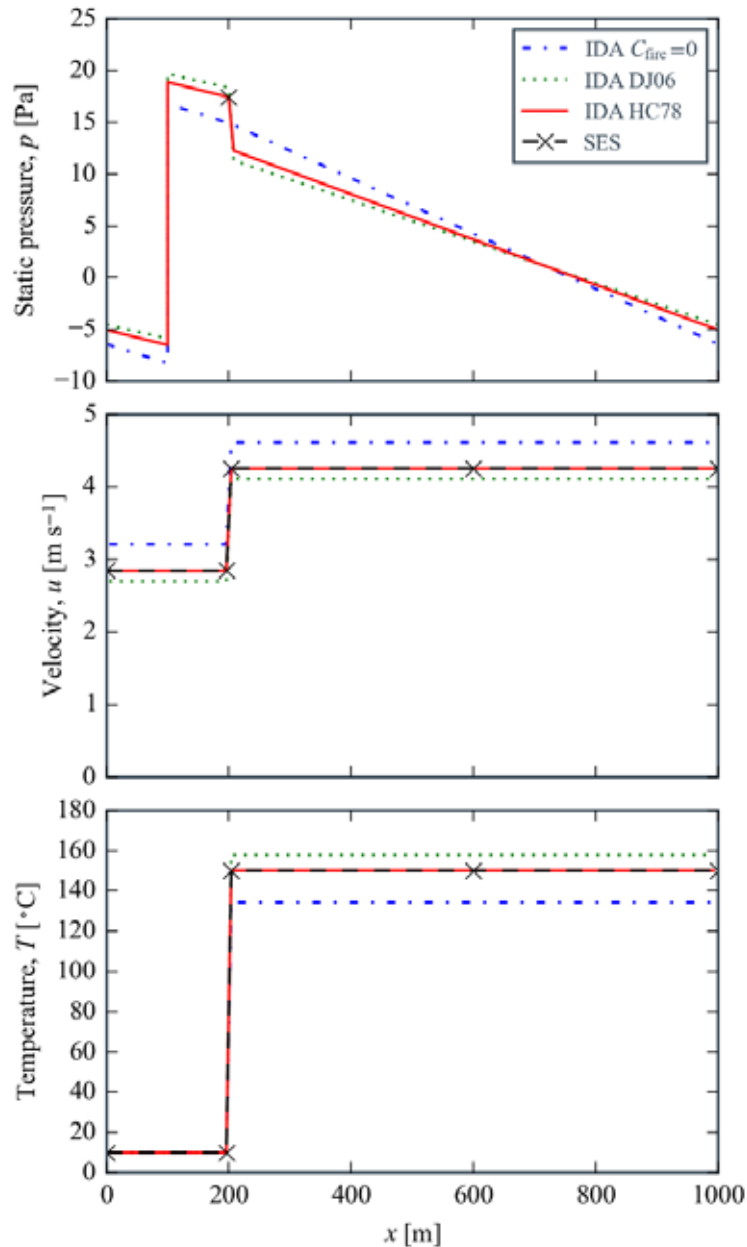
**Figure 3:** Predicted longitudinal profiles of static pressure, velocity and temperature using IDA Tunnel 1.1, where $C_{fire}$ is set at zero as well as via the HC78 and DJ06 models, and using SES, which features the HC78 model

### 3.4. Effect of heat release rate

The implementation of the HC78 model in IDA Tunnel is now compared with SES for heat release rates of 5 MW, 20 MW, 50 MW and 100 MW. The latter two cases require two and four jet fans respectively in order to ensure critical velocity is exceeded.

The pressure change across the fire is presented in figure 4, showing good agreement in all cases. Predictions of static pressure, velocity and temperature profiles were practically identical, with maximum normalised error of 0.4% occurring for static pressure in the 100 MW case (not presented for brevity).
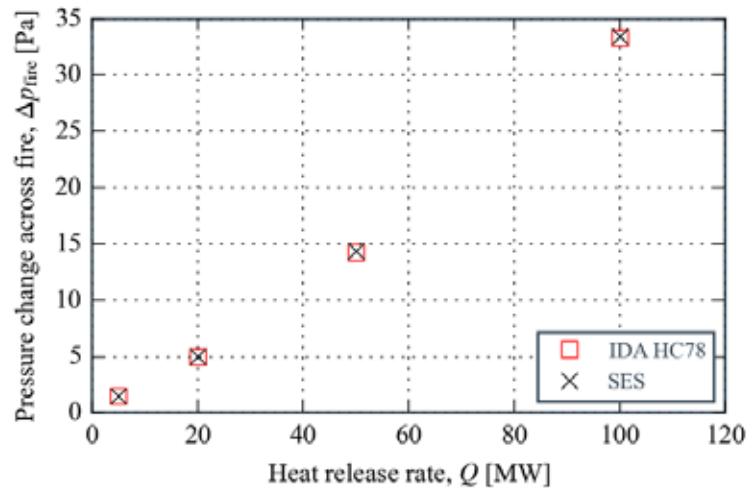
**Figure 4:** Comparison of the pressure change at the fire site for a range of heat release rates

### 3.5.  Effect of wall heat transfer

The effect of wall heat transfer has been eliminated from this study in order to isolate the momentum change across the fire. Solver comparisons which incorporate wall heat transfer have not been considered due to modelling differences and are left to a future study. However, the iterative method of prescribing the pressure change at the fire site, described in section 3.1, has been found to converge well when wall heat transfer is allowed.

### 4.  CONCLUSIONS

A fire increases the aerodynamic resistance of a tunnel through several mechanisms. The increase in velocity downstream of the fire leads to elevated wall friction and local losses, and the momentum change which occurs across the fire causes a corresponding resistance to the upstream flow.

One-dimensional incompressible flow solvers require a correction to the friction and local loss terms to account for fire throttling. An additional loss term is required to account for the momentum change across the fire.

Some flow solvers allow the user to prescribe the pressure drop at the fire. For one such solver, IDA Tunnel 1.1, we propose an iterative method for determining this term, and verify its accuracy through simplified comparisons with another flow solver, SES v4.1.

**REFERENCES**

Dutrieue R, Jacques E (2006) 'Pressure loss caused by fire in a tunnel' in Proc. 12th International Symposium on Aerodynamics and Ventilation of Vehicle Tunnels. BHR Group, UK

EQUA Simulation AB (2014) IDA Tunnel 1.1, http://www.equa.se/en/tunnel/ida-tunnel/ overview

Hwang CC, Chaiken RF (1978) 'Effect of duct fire on the ventilation velocity' US Bureau of Mines Report of Investigations 8311, http://hdl.handle.net/2027/mdp.39015078483404

Hwang CC, Edwards JC (2005) 'The critical ventilation velocity in tunnel fires—a computer simulation' Fire Safety Journal, 40(3):213-44

Kennedy WD, Gonzales JA, Sanchez JG (1996) 'Derivation and application of the SES critical velocity equations' ASHRAE Trans: Research 102(2):40–4

Oka Y, Atkinson GT. (1995) 'Control of smoke flow in tunnel fires' Fire Safety J 25:305–22

U.S. Department of Transportation (2001) 'SES Version 4.1 User's Manual', formerly available from the National Technical Information Service, Springfield, Virginia 22161.

Vaitkevicius A, Collela F, Carvel R (2015) 'Investigating the Throttling Effect in Tunnel Fires' Fire Technology, pp. 1 – 10, DOI:10.1007/s10694-015-0512-z